Electronic Supplementary Material (ESI) for Journal of Materials Chemistry B.

Supporting information

Microfluidic-based modulation of triplet excitons decay in organic phosphorescent nanoparticles for size-assisted photodynamic antibacterial therapy

Cong Chao[#1], Lingling Kang[#1], Wenbo Dai[1], Changsheng Zhao[2], Jianbing Shi[1], Bin Tong[1], Zhengxu Cai*[1], and Yuping Dong*[1]

1. Beijing Key Laboratory of Construction Tailorable Advanced Functional Materials and Green Applications, School of Materials Science and Engineering, Beijing Institute of Technology, Beijing 100081, China

2. Department of Orthopedics, Peking University International Hospital, Beijing 102206, China

# C. Chao and L. L. Kang contributed equally to this work.

Contents

1. Experimental methods

General procedures for the synthesis of guest materials

1,8-naphthalene anhydride (1.00 g, 5.05 mmol) and butylamine (0.74 g, 1.00 ml) were added to a round-bottomed flask containing 20 ml acetic acid and the solution was stirred at 120 ℃ overnight. Then the mixture was poured into ice water. The resulting precipitate was collected by centrifugation, washed with ether and purified on a silica gel column to afford the final product, 1.11 g, 90%.[1]

Measurements of materials

NMR spectra were determined on a Bruker 400 MHz NMR spectrometer using deuterated solvents (d_6-DMSO and $CDCl_3$). UV-vis absorption spectra were performed with a UV-3600 Shimadzu spectrophotometer. Fluorescence and phosphorescence spectra were measured by using FLS1000 lifetime and steady state spectrometer. The total photoluminescence quantum yield of BP/BQD crystalline materials is 15.64%.

Assembly of doped BP/BQD nanoparticles by microfluidic chips

Microchannels with rectangular cross sections were fabricated using typical soft lithography protocols. Channel dimensions were designed with asymmetric structure to control the mixing of two inlets according to Murray's law which states that under ideal conditions, when inlets flow into outlets, the cube of the radius of the inlets should be equal to the sum of the cubes of the radii of outlets. The hydraulic resistance to the liquid flowing in the designed channel has also been evaluated to ensure the flow is smooth without high resistance through the electric circuit analogy which is based on the analogous behavior of hydraulic electric circuits with correlations of pressure to voltage, volumetric flow rate to current, and hydraulic resistance to electric resistance. The benzophenone (BP) and 2-butyl-1*H*-benzo[*de*]isoquinoline-1,3(2*H*)-dione (BQD) have been doped thoroughly as the molar ratio of 100:1. BP/BQD materials (10.00 mg) were dissolved in THF (10 ml). The surfactant (polyethylene-polypropylene glycol, F127, 100.00 mg) was also added into the THF solution. The THF solution with the concentration of 1 mg/ml was pumped by Teflon tubing into one inlet of the

microfluidic chip (width: 150 μm, height: 150 μm and length: 1.5 cm). Deionized (DI) water was pumped into another inlet of the microfluidic chip (width: 150 μm, height: 150 μm and length: 1 cm). When the organic solution met DI water at the bifurcation of the microfluidic channels, the doped BP/BQD nanoparticles were self-assembled with the decrease of good solvent, and then flowed from the outlet microchannel(width: 300 μm, height: 300 μm and linear length: 3 cm). THF was removed by evaporation under a fume hood overnight. The flowrate of two inlets can be precisely controlled by the syringe pumps, and through varying the flowrate ratio of two inlet fluids, the size of doped BP/BQD nanoparticles can be tuned. The size range of BP/BQD nanoparticles synthesized by this microfluidic chip is approximately 20 to 600 nm due to the limitation of channel dimension and pump flowrate setting.

Nanoprecipitation approach The doped BP/BQD material (1.00 mg) and F127 (10.00 mg) were dissolved in THF (1 ml). Then, the doped BP/BQD nanoparticles were prepared by quickly injecting THF solution into DI water (10 ml) under ultrasonication (300 W) for 20 mins to remove the organic solvent.[2]

Dynamic light scattering (DLS) The hydrodynamic particle size, size distribution, and zeta potential of nanoparticles suspension in DI water were measured by using DLS (Nicomp 380 Z3000, USA), and three measurements for every nanoparticle sample have been conducted.

X-ray diffraction (XRD) X-ray diffraction was conducted by using a Rigaku MiniFlex X-ray diffractometer to characterize the crystallinity of BP/BQD NPs and BP/BQD con-NPs.

Transmission electron microscopy (TEM) Suspensions of the doped nanoparticles were drop-cast onto TEM grids and allowed to air dry under ambient conditions, then TEM images were taken by using (JEM2100f) to characterize the morphology of the doped nanoparticles. Selected-area electron diffraction pattern of doped nanoparticles has also been imaged to characterize the crystallinity of the nanoparticles.

Bacterial culture Gram-negative *E. coli* (ATCC 25922) and Gram-positive *S. aureus* (ATCC 25923) were purchased from Shanghai Fuxiang Biotechnology Co. Ltd (Shanghai, China). The strains were used for antibacterial experiments in the following

researches and stored at -80 ℃. The microbes were revived in Luria-Bertani (LB) broth medium at 37 ℃ overnight, and the strains were purified by plate streaking method on the surface of agar solid medium. A single colony of *S. aureus* on Luria-Bertani (LB) solid agar plates was incubated into 10 mL liquid LB broth medium and grown overnight at 37 ℃ in a shaking incubator at 180 rpm. The bacteria that have grown to the logarithmic growth phase were harvested and washed 3 times with PBS (10 mM, pH=7.4) by centrifugation (8000 rpm for 3 min). The supernatant was discarded, and the remaining *S. aureus* were re-suspended in PBS. The concentration of bacterial cells was determined by measuring the optical density of bacterial suspensions at 600 nm with a Multiskan SkyHigh microplate spectrophotometer (Thermo Fisher Scientific, USA), and regularized to the desired concentrations with PBS before being used. As for *E. coli* (Gram-negative bacteria), the experimental conditions and operations are exactly the same as that of *S. aureus*.

Antibacterial tests of NPs against different microbes Freshly prepared bacteria were diluted with PBS to 10^8 CFU·mL^{-1}. 10^{-6} M NPs of different particle sizes (105, 125, 140, 190, 220, 250 and 280 nm) were added to the microbial suspension. The mixture was incubated at 37 ℃ for 1 h, followed by exposing to white light irradiation (5 mW·cm^{-2}) for 15 min, and the pathogen suspensions were serially diluted 10^5-fold with PBS. Then, 100 μL of the mixed solution was spread on LB-agar plate with a diameter of 90 mm and cultured for another 24 h in a 37 °C biochemical incubator to form colonies before being counted and taken photos. The number of colony-forming units (CFU) of diluted microorganism solutions was determined by the standard plate counting method. The bacterial inhibition ratio (IR) was calculated according to the following equation:

$$IR = \frac{C_0 - C}{C_0} \times 100\%$$

where C is the CFU of the experimental group treated by NPs, and C_0 is the CFU of the control group without incubation with NPs.

The experimental conditions and operation of the bactericidal effect of NPs with different concentrations (4×10^{-5}, 2×10^{-5}, 1×10^{-5}, 5×10^{-6}, 2.5×10^{-6}, 1.25×10^{-6}, 10^{-6}, 10^{-7},

10^{-8} M) are basically the same as the above experimental steps.

Reactive oxygen species (ROS) detection 2′, 7'-dichlorodihydrofluorescein diacetate (DCFH-DA) was used as a ROS indicator to confirm the generation of ROS in doped NPs suspension. Here is the detailed instruction: The DCFH-DA solution (final concentration is 1 mM) was prepared by adding DCFH-DA (1 mg) into absolute ethyl alcohol (2 mL). Ethanol solution of DCFH-DA (500 μL, 1 mM) and aqueous solution of NaOH (2 mL, 10 mM) were mixed in the dark at room temperature for 30 min. Subsequently, 10.0 mL of PBS (25 mM) was added to obtain 40 μM 2′,7′-dichlorodihydrofluorescein (DCFH) solution. An aqueous doped NPs solution (10 μM final concentration) with different particle size (105, 140 and 220 nm) was added into the activated DCFH solution (1 μM final concentration). The solution was shook at room temperature for 1 min in the dark, followed by UV light irradiation (5 $mW \cdot cm^{-2}$) with the time interval of 1 min. The activated DCFH solution irradiated by UV light (5 $mW \cdot cm^{-2}$) with the time interval of 1 min was used as the control. The non-fluorescent DCFH could be further oxidized into the fluorescent 2′,7′-dichlorofluorescein (DCF) in the presence of ROS. Thus, the fluorescence intensity of DCF could represent the amount of ROS. The fluorescence spectra (500-700 nm) of DCF was then measured with the excitation wavelength of 480 nm. Then the relative emission intensity ($I/I_0 - 1$) at 525 nm versus irradiation time was plotted to compare the production capacity of ROS.

The measurement of ROS under white light (5 $mW \cdot cm^{-2}$) irradiation is mostly consistent with the above experimental conditions and procedures.

Detection of $^1O_2$ Generation by SOSG $^1O_2$ generation in solution were monitored with SOSG via its PL intensity. Briefly, SOSG in methanol (working concentration: 10 μM) was mixed with the BP NPs, BQD NPs, and BP/BQD NPs with different particle size solution (working concentration: 10 μM) and irradiated by 365 nm UV light (5 $mW \cdot cm^{-2}$). Then, the PL intensities at 540 nm for every minute were recorded in a PL spectrofluorometer (Excitation wavelength: 488 nm).

Electron paramagnetic resonance (EPR) EPR experiments were conducted at room temperature in a quartz capillary (I.D. 1.50 mm and O.D. 1.80 mm). Continuous wave EPR spectra were collected at Bruker Elexsys E580-X EPR spectrometer, which was used to identify the type of ROS using 5,5-Dimethyl-1-pyrroline N-oxide (DMPO) as the radical indicator. Samples were prepared by mixing 50 μL, 100 μM of BP NPs, BQD NPs and BP/BQD NPs in water and 10 μL of DMPO (200 mM) in water, respectively. The samples were prepared in the dark for dark-condition test, then, samples were exposed to white light irradiation at 0.18 $W \cdot cm^{-2}$ for 3 minutes before recording signals by EPR.

Evaluation of photodynamic antibacterial effect of doped NPs Microorganisms solution was irradiated by a 365 nm UV lamp (1 $mW \cdot cm^{-2}$) for 15 min after incubating with 10^{-6} M doped NPs for 1 h. Two control groups were prepared for comparisons, including samples only treated with UV light in the absence of doped NPs and only incubated with doped NPs without UV light irradiation, respectively. Then, 10 μL bacterial suspensions from the above *S. aureus* or *E. coli* suspensions were serially diluted 10^5-fold to LB broth medium according to a doubling dilution method. Subsequently, 100 μL bacterial suspension was uniformly spread on LB agar plate and cultivate for another 20 h in a 37 °C biochemical incubator. The images of clone plates were taken before counting. Each group had three replicates. The bacterial inhibition ratio (IR) was calculated according to the following equation:

$$IR = \frac{C_0 - C}{C_0} \times 100\%$$

where C is the CFU of the experimental group treated by doped NPs, and C_0 is the CFU of the control group without incubating with doped NPs.

Scanning electron microscopy (SEM) assay To confirm the antibacterial performance of the doped NPs and the morphological changes of bacterial cells, SEM studies were carried out based on a previous report.[3] 1 mL of logarithmic growth phase bacterial cells solution containing 10^6 $CFU \cdot mL^{-1}$ was combined with an equal volume of NPs with the concentration of 10^{-6} M. Then, the bacterial suspension was incubated on a

constant temperature shaker at 37℃ for 2 h. The control group was cultured in LB broth at 37 ℃ for the same time. After cultivation, the bacteria were collected by centrifugation (6000 rpm for 3 min) and fixed with 2.5% glutaraldehyde at 4 ℃ overnight. The microbes were rinsed with PBS three times after fixation. Subsequently, the bacteria were subjected to gradient dehydration for 20 min with different concentration ethanol (30%, 50%, 70%, 80%, 90%, 95% and 100%). After dehydration, the bacterial suspension was placed on a clean silicon wafer followed by air drying. After the samples were wholly dried, gold was sprayed before being observed by a scanning electron microscope (SEM, Japan, RegulusS8230) at an accelerating voltage of 15 kV.

LIVE/DEAD bacterial cells staining experiment Molecular Probes' LIVE/DEAD® *Bac*Light™ Bacterial Viability Kits provide a two-color fluorescence assay of bacterial viability that distinguish live (green fluorescence) and dead (red fluorescence) bacterial cells. The bacterial suspension (OD_{600} = 0.1, 500 μL) was mixed with equal volume (500 μL) of BP/BQD NPs in PBS at a final concentration of 10^{-6} M, which was added to a tube and cultured in shaker at 37 °C for 1 h and centrifuged at 5000 rpm for 3 min to remove cell free supernatant. Besides, a control group which the bacteria treated with PBS only was prepared for comparison. Next, the mixture of SYTO 9 and propidium iodide (PI) were added to the above microbial solutions at final concentrations of 20 μM and 4.5 μM, respectively. Then the solutions were further incubated in the dark at 37 °C for 30 min, and bacterial cells were collected by centrifugation and rinsed 3 times with PBS and another 100 μL of PBS was added. The bacterial solution (5 μL) was added onto a glass slide, which was immobilized by a clean coverslip which is used for fixation. Afterwards, live/dead bacterial cells were observed by CLSM (SYTO 9, Ex = 485 nm, Em = 490-540 nm; PI, Ex = 485 nm, Em = 630-680 nm) using an oil immersed 100 × objective lens.

In vitro cytotoxicity 3T3 cells (murine fibroblast cell line) were obtained from National Infrastructure of Cell Line Resource (NICR), cultured with in RPMI-1640 media containing 10% FBS and 2% penicillin-streptomycin at 37 °C in a humidified atmosphere of 5% CO_2.

The 3T3 cells (1×10^4 cells/well) were cultured in 96-well plates, with three duplicate wells in each group. After 12 h, the cells were cultures with BP/BQD nanoparticles at different concentrations and sizes for 30 min. Then the medium was discarded, and the fresh medium was added to each well for further incubation for 24 h. The cells were incubated with MTS solutions (5 mg/mL) for 3 h at 37 °C. The absorbance of each well was measured at 490 nm by a microplate reader (BioTek).

Statistical analysis All quantitative data were expressed as mean ± standard deviation (SD). Number of samples for each statistical analysis was 3 trials per group. Statistical analyses were conducted using Student's t-test by Graphpad prism 8 software. Values of $*p < 0.05$, $**p < 0.01$ and $***p < 0.001$ were considered statistically significant.

2. Figures and tables

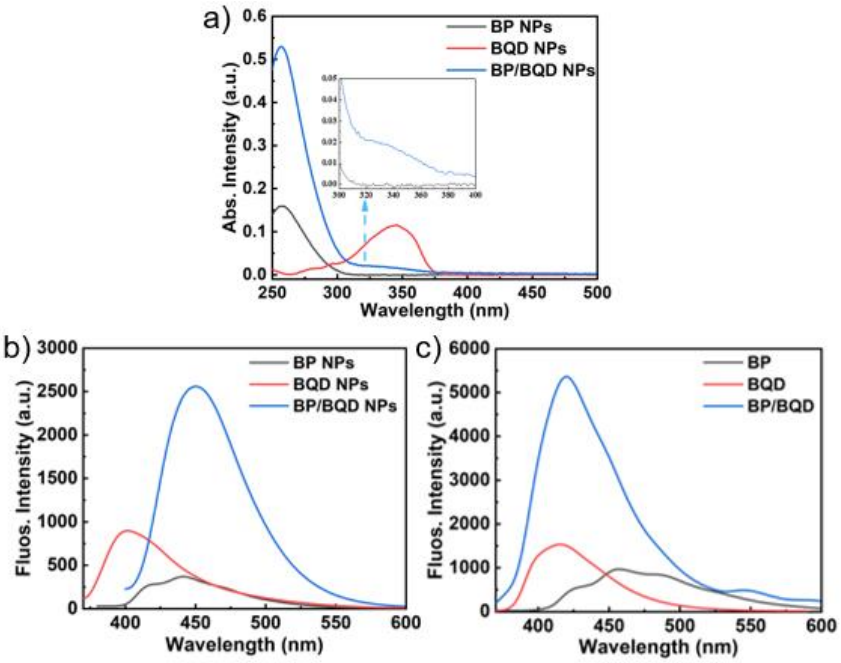

Figure S1 (a) UV-vis absorption spectra and emission spectra of the host (BP), the guest (BQD), and host-guest (BP/BQD) materials; (b) Fluorescence spectra of the host nanoparticles, the guest nanoparticles and the host-guest nanoparticles dispersed in DI water, concentration: 1×10^{-5} M; (c) Fluorescence spectra of the host materials, the guest materials and the host-guest crystalline materials.

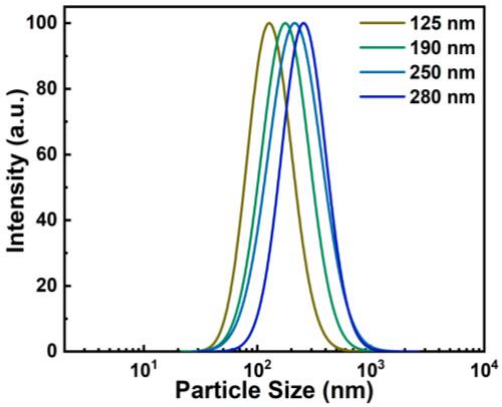

Figure S2 DLS measurement of BP/BQD NPs suspensions prepared through microfluidic technology with different particle size in DI water, the poly-dispersity indexes are 0.12, 0.14, 0.11, and 0.16 for the sizes of 125 nm, 190 nm, 250 nm and 280 nm, respectively.

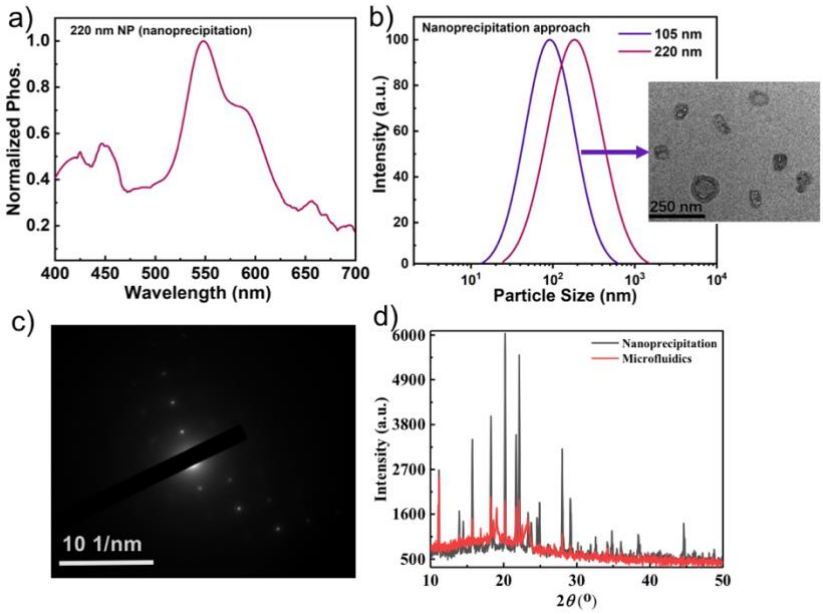

Figure S3 Characterization of BP/BQD con-NPs prepared through conventional nanoprecipitation. (a) phosphorescence spectrum of BP/BQD con-NPs suspension; (b) DLS measurement of BP/BQD con-NPs suspensions, the poly-dispersity indexes are 0.52 and 0.55 for the sizes of 105 nm and 220 nm, respectively. Insert: TEM image of BP/BQD con-NPs; (c) selected-area electron diffraction pattern of BP/BQD con-NPs with the size of 105 nm; (d) XRD patterns of BP/BQD NPs and BP/BQD con-NPs.

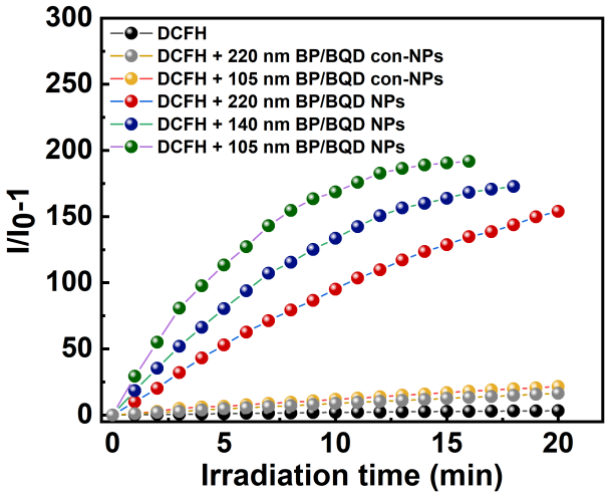

Figure S4 Comparison of the total ROS generating efficiency of BP/BQD nanoparticles assembled through conventional nanoprecipitation (BP/BQD con-NPs) and microfluidic technology (BP/BQD NPs) with different particle sizes under the UV light irradiation. 2,7-dichlorodi-hydrofluorescein diacetate (DCFH-DA) is the probe.

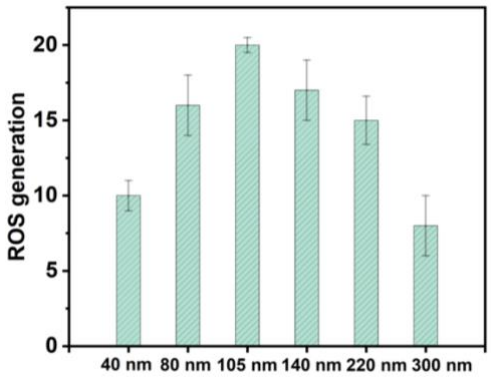

Figure S5 Comparison of the total ROS generation (vs DCFH) of BP/BQD NPs with different sizes under the UV light irradiation, 2,7-dichlorodi-hydrofluorescein diacetate (DCFH-DA) is the probe.

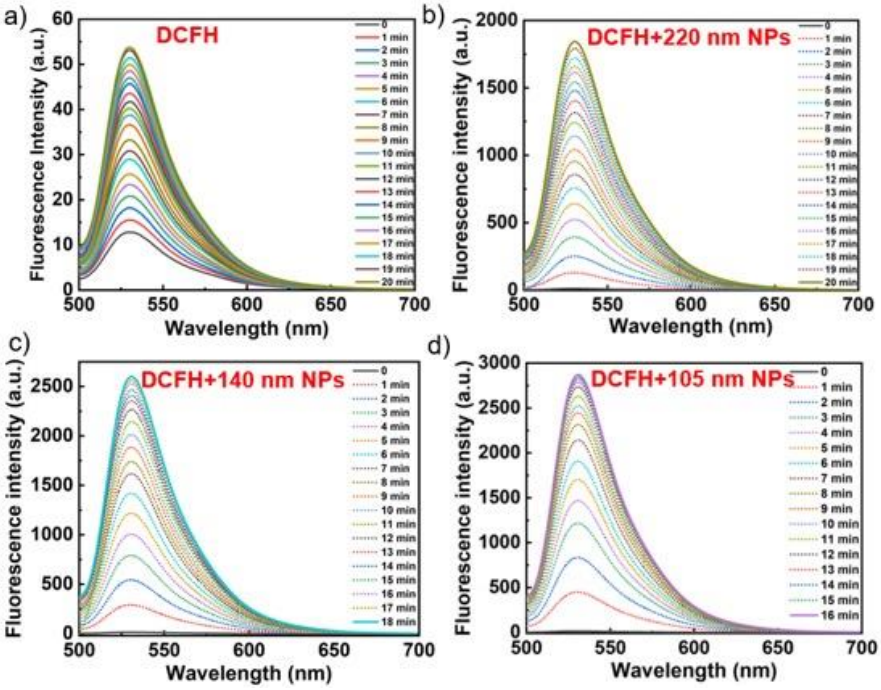

Figure S6 Fluorescence intensity of (a) DCFH, and with the addition of BP/BQD NPs with the sizes of (b) 220 nm, (c) 140 nm and (d) 105 nm with the exposure to UV light.

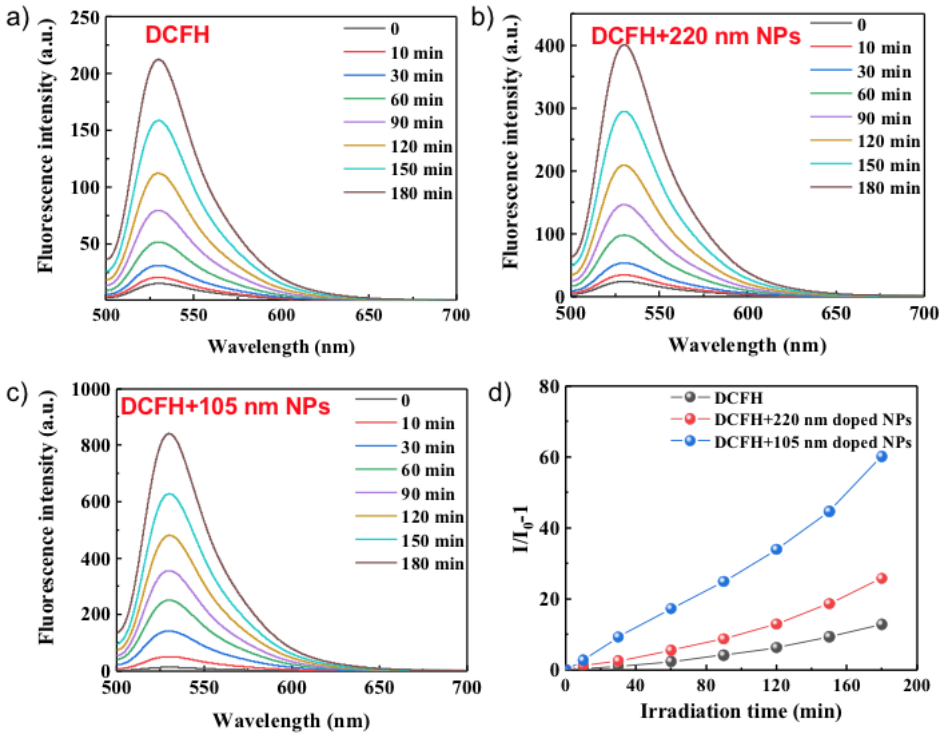

Figure S7 Fluorescence intensity of (a) DCFH, and with the addition of BP/BQD NPs with the sizes of (b) 220 nm and (c) 105 nm with the exposure to white light; (d) comparison of the total ROS generating efficiency of BP/BQD NPs with different

particle sizes under white light irradiation.

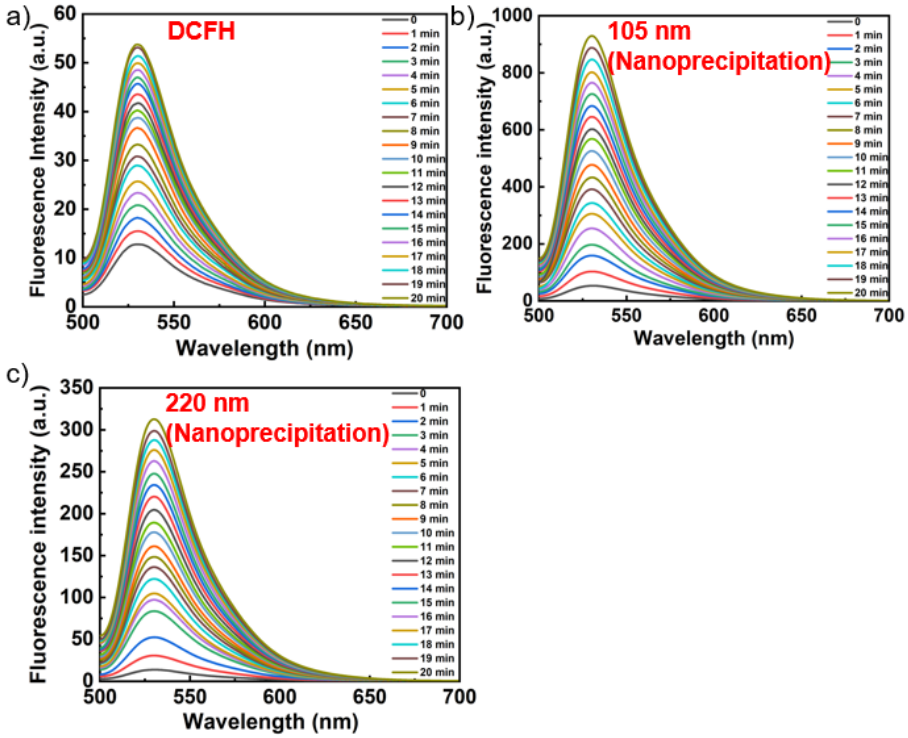

Figure S8 ROS generation efficacy of BP/BQD nanoparticles prepared by conventional nanoprecipitation approach (BP/BQD con-NPs). Fluorescence intensity of (a) DCFH, and with the addition of BP/BQD con-NPs with the sizes of (b) 105 nm and (c) 220 nm with the exposure to UV light.

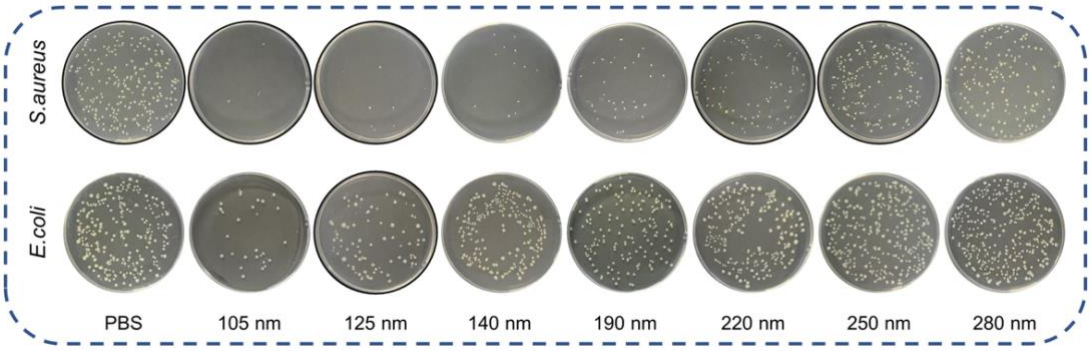

Figure S9 Antibacterial evaluation *in vitro*, photographs of plate agars spread with *S. aureus* and *E. coli* treated with BP/BQD NPs. The concentration is about 10^{-6} M, the incubation time is 1 h.

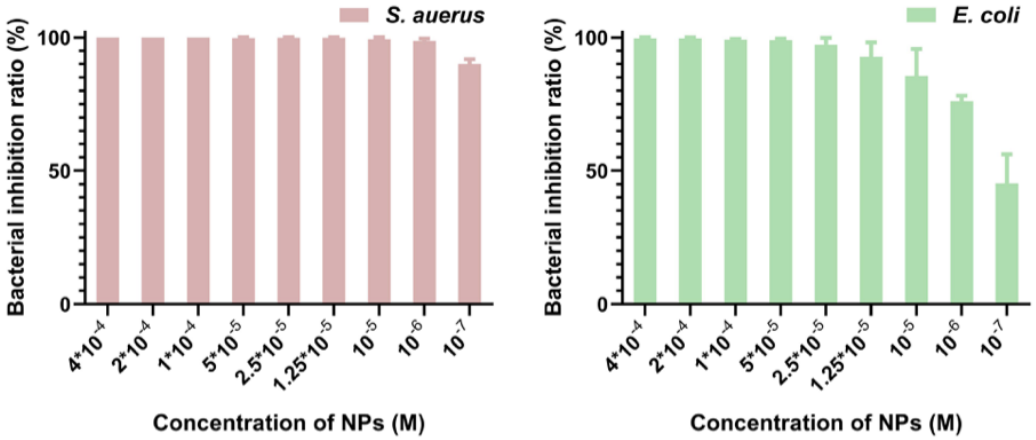

Figure S10 Concentration-dependent antibacterial activity of BP/BQD NPs with the size of 105 nm, the incubation time is 1 h. The error is the standard deviation from the mean.

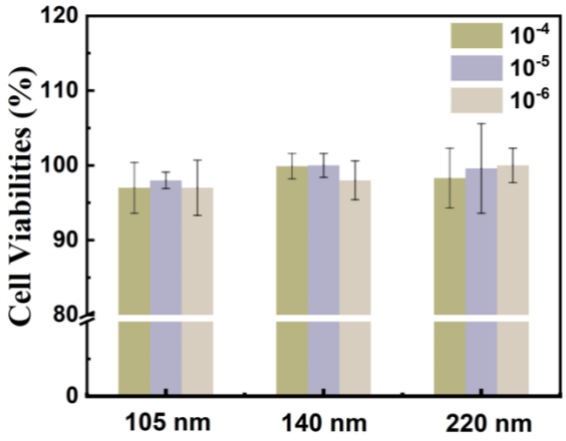

Figure S11 The percentage of 3T3 cell viability in the presence of BP/BQD NPs with the size of 105 nm, 140 nm and 220 nm, without light irradiation. All bars represent mean ±SD (n=3).

Table S1 Properties of the host, guest, and doped nanoparticle suspensions synthesized by the microfluidic device

NP	Size (nm)	Zeta potential (mV)
Host NPs	120±5	-12.38±0.05

Guest NPs	125±5	-10.43±0.05
Doped NPs	130±5	-19.20±0.10

Derivation of biophysical model

The real biological bacterial surface can be simplified as an infinite elastic film.[4] The interaction of BP/BQD nanoparticles with bacterial cell surface is determined by the contact area of the adsorbed nanoparticles. Local stretching and compression of the bacterial cell wall is balanced by the energy gain attributed to the attraction force and the energy loss attributed to the stretching and compression force. According to Ivanova et al,[5] the surface tension of bacterial surface (δ) can be calculated by

$$\delta = k\frac{S-S_i}{S_i} \quad \text{Equation (S1)}$$

$$\int \frac{d\sigma}{1+\alpha(r)} = S_i \quad \text{Equation (S2)}$$

where k is the elastic modulus of bacterial cell wall, S_i is the initial surface area and S is the actual surface area of the bacterial cell wall with the adsorption of NPs. $d\sigma$ is the element of the BP/BQD nanoparticles surface, and $\alpha(r)$ is the local stretching force at the point r of the bacterial cell wall. k is a constant for a certain bacteria strain.

As the aggregation of BP/BQD nanoparticles is difficult to avoid, the interaction between BP/BQD aggregates and individual BP/BQD nanoparticles with bacterial cell wall was both considered in this modelling. It is assumed that D(N) is the distribution of BP/BQD aggregates. The radius of a spherical aggregate (r_A) is assumed to be related to the individual NPs radius (r), and the surface density of aggregates (μ_{agg}) is given by,

$$\mu_{agg} = \mu_i(\frac{r_A}{r})^{-3} \quad \text{Equation (S3)}$$

where μ_i is the surface density of adsorbed individual NP on the bacterial cell wall.

Considering the steric effect among aggregates, the free energy of aggregates is given by Equation S4 to achieve the equilibrium distribution of BP/BQD aggregates,

$$G = k_B T \sum_{N=1}^{\infty} D(N)[lnD(N) - 1 + Ng_N] \quad \text{Equation (S4)}$$

where g_N is the energy for BP/BQD aggregates containing N nanoparticles, k_B is the Boltzmann constant, and T is the temperature. The energy g_N for a spherical aggregate is calculated by: $g_N = g_\infty^0 + \frac{\varphi}{N^{1/3}}$. g_∞^0 is the bulk energy, and φ is the cohesive energy among BP/BQD nanoparticles.

Based on Equations S1-S4, the surface tension for BP/BQD aggregates can be given as

$$\delta = kr^2\left(\beta N^{\frac{2}{3}} - 1\right)\mu/N \qquad \text{Equation (S5)}$$

with the assumption that the radius of the BP/BQD aggregate is related with the radius of single nanoparticles. The parameter β has been introduced in this modelling to characterize the interaction between BP/BQD nanoparticles and the bacterial cell surface per adsorption site, which can be mathematically related to the angle θ (see Figure S12). Therefore, Equation (S6) can be written as,

$$\delta = k\left[\frac{2-2cos\theta}{sin^2\theta \cdot N} - \frac{{r_A}^2(2-2sin\theta)}{r^2 N^{\frac{5}{3}} sin^2\theta}\right] \qquad \text{Equation (S6)}$$

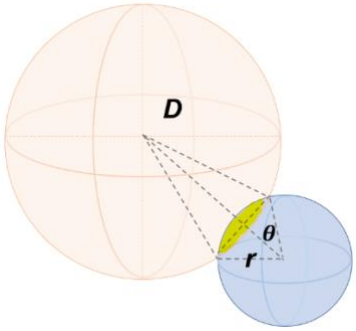

Figure S12 Schematic representation of single nanoparticle adhered onto the surface of the bacterial cell wall, and the nanoparticle size has been exaggerated for clarity.

NMR spectra and Mass spectrometry

^{1}H NMR (400 MHz, DMSO) δ 8.38 - 8.33 (m, 4H), 7.79 - 7.75 (t, J = 8.0 Hz 2H), 3.99 - 3.95 (t, J = 8.0 Hz, 2H), 1.60 - 1.53 (m, 2H), 1.37 - 1.27 (m, 2H), 0.92 - 0.88 (t, J = 8.0 Hz 3H). ^{13}C NMR (100 MHz, $CDCl_3$) δ 164.19, 133.81, 131.57, 131.14, 128.14, 126.91, 122.76, 40.26, 30.24, 20.41, 13.87. High resolution ESI-MS (m/z): $C_{16}H_{15}NO_2$ for $[M]^+$, calculated 254.1103, found 254.1155.

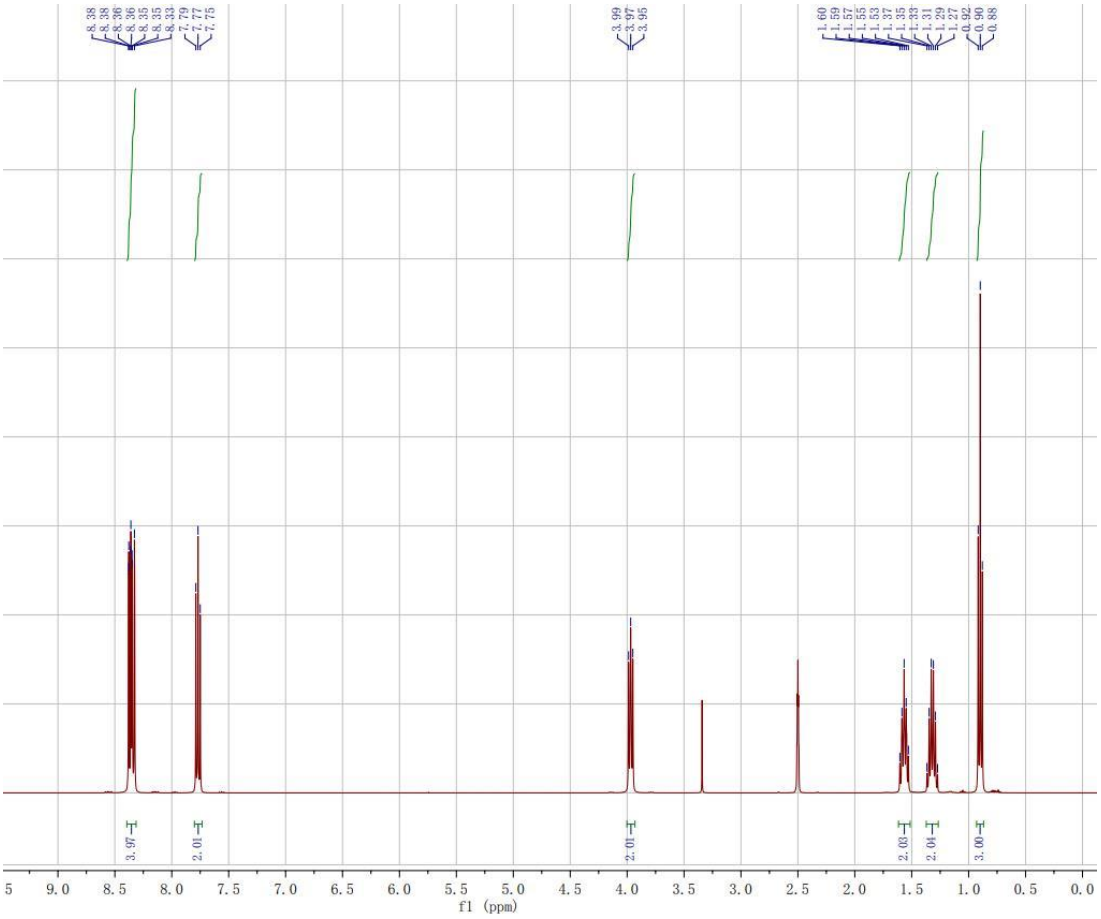

Figure S13 ^{1}H-NMR spectrum of BQD.

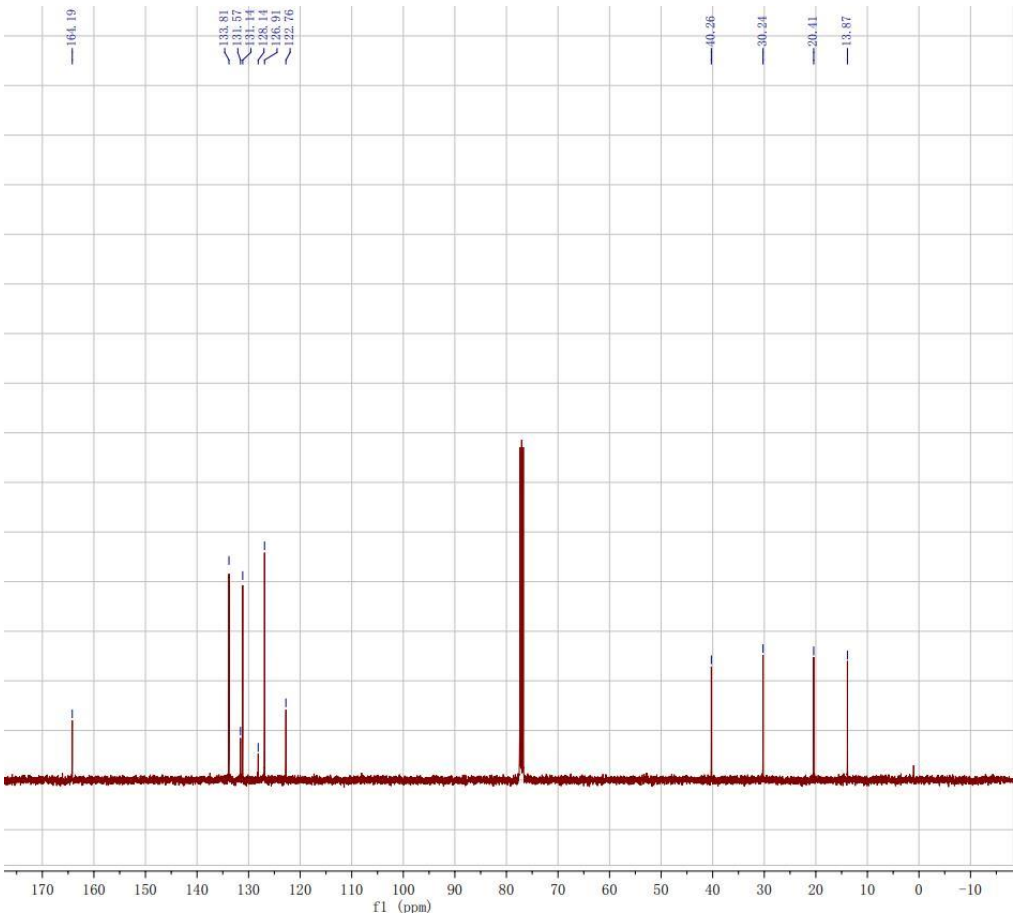

Figure S14 ^{13}C-NMR spectrum of BQD.

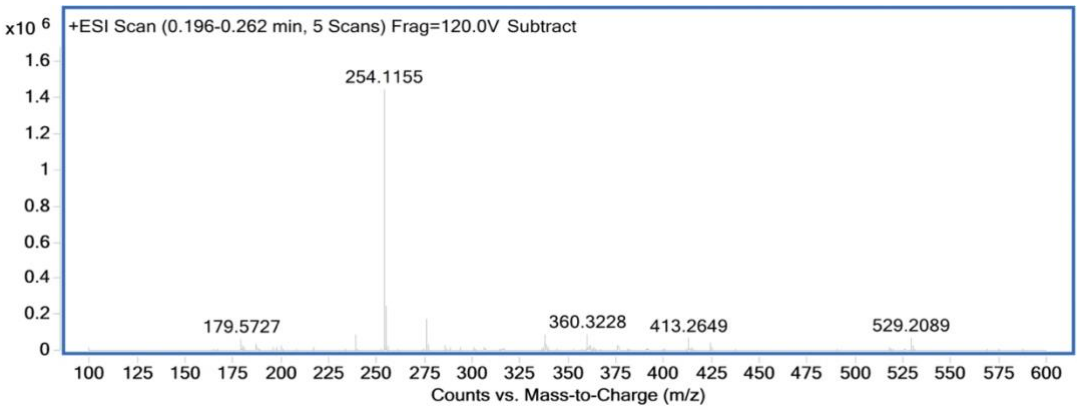

Figure S15 Mass spectrum of BQD.

Reference

1. Chen, X.; Xu, C.; Wang, T.; Zhou, C.; Du, J.; Wang, Z.; Xu, H.; Xie, T.; Bi, G.; Jiang, J.; Zhang, X.; Demas, J. N.; Trindle, C. O.; Luo, Y.; Zhang, G., Versatile Room-Temperature-Phosphorescent Materials Prepared from N-Substituted Naphthalimides: Emission Enhancement and Chemical Conjugation. *Angew Chem Int. Ed.* **2016,** *55* (34), 9872-9876.

2. Qin, W.; Alifu, N.; Lam, J. W. Y.; Cui, Y.; Su, H.; Liang, G.; Qian, J.; Tang, B. Z., Facile Synthesis

of Efficient Luminogens with AIE Features for Three-Photon Fluorescence Imaging of the Brain through the Intact Skull. *Adv. Mater.* **2020,** *32* (23), 202000364.

3. Xie, T.; Qi, Y.; Li, Y.; Zhang, F.; Li, W.; Zhong, D.; Tang, Z.; Zhou, M., Ultrasmall Ga-ICG nanoparticles based gallium ion/photodynamic synergistic therapy to eradicate biofilms and against drug-resistant bacterial liver abscess. *Bioact. Mater.* **2021,** *6* (11), 3812-3823.

4. Mathelié-Guinlet, M.; Grauby-Heywang, C.; Martin, A.; Février, H.; Moroté, F.; Vilquin, A.; Béven, L.; Delville, M.-H.; Cohen-Bouhacina, T., Detrimental impact of silica nanoparticles on the nanomechanical properties of Escherichia coli, studied by AFM. *J. Colloid Interf. Sci.* **2018,** *529*, 53-64.

5. Linklater, D. P.; Baulin, V. A.; Le Guével, X.; Fleury, J. B.; Hanssen, E.; Nguyen, T. H. P.; Juodkazis, S.; Bryant, G.; Crawford, R. J.; Stoodley, P.; Ivanova, E. P., Antibacterial Action of Nanoparticles by Lethal Stretching of Bacterial Cell Membranes. *Adv. Mater.* **2020,** *32* (52), 2005679.